Environ Earth Sci (2016) 75:672
DOI 10.1007/s12665-016-5506-8

THEMATIC ISSUE

Iron biogeochemistry in Holocene palaeo and actual salt marshes in coastal areas of the Pampean Plain, Argentina

M. Osterrieth[1,2] · N. Borrelli[1,2,3] · M. F. Alvarez[1,2,3] · G. N. Nóbrega[4] · W. Machado[5] · T. O. Ferreira[4]

Received: 30 May 2015 / Accepted: 25 February 2016 / Published online: 11 April 2016

Abstract In salt marshes, the hydrodynamics and the availability of iron, organic matter and sulphate, influence the formation and/or dissolution of iron sulfides and iron oxyhydroxides. Therefore, they constitute key factors affecting the iron biogeochemical processes in these environments. The aim of this work is to evaluate the physicochemical and mineralogical variations associated to iron biogeochemistry in palaeo and actual salt marshes in the area of influence of the Mar Chiquita coastal lagoon, Pampean Plain, Argentina. In soils of exhumed palaeo marshes, the iron contents are 56–95 μmol g^{-1}, whereas these contents decrease to 36–75 μmol g^{-1} in actual marsh soils. The presence of framboidal and poliframboidal pyrites associated with gypsum, barite, calcite, halite and iron oxyhydroxides defines the conditions of the pedosedimentary sequences of the Holocene paleomarshes. Sequences of pyrite formation (sulfidization) and degradation (sulfuricization) were observed. These processes were evidenced by a sequential extraction, reflecting that the largest proportion of iron is in the form of crystalline iron oxides (28–76 %) and lepidocrocite (6–16 %); while the proportion associated with ferrihydrite and pyrite is low (0–9 and 1–17 %, respectively). These facts could be partly explained by the complex redox processes characteristic of these environments, such as aeration generated by the rhizosphere and intense bioturbation by invertebrates. These iron biomineralizations have been useful because they allow paleoenvironmental interpretations and characterization of paleomarshes, and environmental inferences related to the management of actual salt marshes.

Keywords Biomineralization · Framboidal and poliframboidal pyrites · Sequential extraction · Coastal wetlands

Introduction

Salt marshes are one of the most productive systems of the world (Odum 1970; Duarte et al. 2005); they are widely urbanized zones and occupy large coastal areas. They are transitional ecosystems that couple continental and marine environments (Viaroli et al. 2007), where major changes in water chemistry, sediment composition and biology can occur on small spatial and temporal scales (Bianchi 2006). Because of that, soils in estuarine environments are complex systems that result from interactions between abiotic (e.g., tides and physiography) and biotic (activities of plants, invertebrates and microorganisms) factors, which may change within short distances (Ferreira et al. 2010); in concordance with the pedological processes of additions, transformations, transfers and removals defined by Simonson (1959).

✉ N. Borrelli
nlborrel@mdp.edu.ar

1 Instituto de Geología de Costas y del Cuaternario (IGCyC), FCEyN, UNMdP-CIC, CC 722 (7600), Mar Del Plata, Buenos Aires, Argentina

2 Instituto de Investigaciones Marinas y Costeras (IIMyC), CONICET-UNMdP, Mar Del Plata, Buenos Aires, Argentina

3 Consejo Nacional de Investigaciones Científicas y Técnicas (CONICET), Buenos Aires, Argentina

4 Departamento de Ciencia do solo, Escola Superior de Agricultura Luiz de Queiroz (ESALQ), Universidade de São Paulo (USP), Sao Paulo, Brazil

5 Departamento de Geoquímica, Instituto de Química, Universidade Federal Fluminense, Niteroi, Brazil

Soils developed in salt marshes are characterized by high organic matter contents and tidal flooding, and play an important role in the biogeochemical cycling of iron (Fe) and sulfur (S) (Tobias and Neubauer 2009). In anoxic soils of salt marshes, the bacterial sulfate reduction (BSR) may be one of the main processes in the mineralization of organic matter (Howarth 1984). When favorable conditions to the BSR occur (e.g., abundant supplies of sulfate; organic matter; and reactive Fe from active hydrological systems, rivers and tides), some metastable Fe sulfides are formed and accumulated such as amorphous FeS, mackinawite (FeS), greigite (Fe_3S_4) and pyrrhotite (FeS) (Morse et al. 1987). These iron sulfides can be later transformed to pyrite (FeS_2), mainly in framboidal pyrite form (Berner 1970; Osterrieth 1992; Tobias and Neubauer 2009).

As framboidal pyrite is mainly the result of a biological metabolic process, it is included within the process of biologically induced mineralization, also called biomineralization (Lowenstam 1981; Lovley 2000). Because pyrite is thermodynamically the most stable end product of the bacterial sulfate reduction (Berner 1984), it is widely used as biogeochemical proxy to reconstructing geological events and identifying periodically changing environmental redox conditions (Henderson 2002; Ferreira et al. 2015). This pyrite applicability as a proxy to identify a variety of redox controlled cyclic transitions in depositional environments is due to its stability (Raiswell and Berner 1985), allowing interpretations on the factors that control its formation and accumulation during early diagenesis, including availability of iron, sulfate, organic carbon and hydrodynamics (Berner 1970, 1982, 1984).

Knowledge of the evolution of palaeomarshes is critical to understand the processes acting in the actual marshes, especially considering urban development in coastal areas and the consequences that different human activities could have, considering the active iron biogeochemistry and the possible acidification processes generated by the oxidation of iron sulfides (Polastro 1981).

In Argentina, the first report about the biomineralization of framboidal pyrite associated with palaeo salt marshes environments was in 1992 (Osterrieth 1992), without further information; while there are a large number of reports of the pyrite formation and its biogeochemical implications in salt marshes ecosystems in other regions (Stribling 1997; Wilkin et al. 1996; Roychoudhury et al. 2003; Ferreira et al. 2010; Koretsky et al. 2003; Otero and Macias 2003; Otero et al. 2006; Tobias and Neubauer 2009).

In the Pampean Plain, coastal morphodynamics throughout the Holocene has been very active, producing variations linked to the installation of coastal barriers that determine the evolution of both palaeo and actual marsh (Isla et al. 1988; Violante et al. 2001), and dunes which have fully or partially buried ancient coastal lagoons. For this reason, and because Mar Chiquita Coastal Lagoon is a unique type of environment in Argentina, the aim of this work is to evaluate the physico-chemical and mineralogical variations associated to iron biogeochemistry in palaeo and actual salt marshes in the area of influence of the Mar Chiquita coastal lagoon, Pampean Plain, Argentina. Although the presence of framboidal pyrite is frequently reported for soils of tidal flats, coastal marshes and swamps from tropical to subtropical environments of Southeast Asia, Africa and South America, this work is the first report of its presence in the southeast Pampean Plain.

Materials and methods

Study area

The site under study is located in the Mar Chiquita district, Province of Buenos Aires (37°8′10″–37°51′S and 58°5′40″–57°11′4″W) (Fig. 1a). This area is part of the depressed Pampa (Tricart 1973) where four geomorphological areas are distinguished (Schnack and Gardenal 1979): (a) Coastal dunes, (b) Marginal plain, (c) Shell ridges, (d) Continental deposits. The parent materials of soils conform four stratigraphic units: (1) Faro Querandí Formation: coastal dunes; (2) Mar Chiquita Formation: ingressive deposits, which are distinguished: beach facies, shell cordon and coastal lagoon facies, sandy-clay sediments greenish gray, with shell fragments; (3) Santa Clara Formation: continental deposits (pampean loess and silts (Frenguelli 1950); (4) Silts Nahuel Ruca Formation: silty dunes around Hinojales and Nahuel Rucá lakes. Soils in the study area belong to different series, dominated by typic Udipsaments, aquic Hapludolls, typic Peluderts, fluventic Hapludolls, thaptoargic Hapludolls, typic Natraquolls and haplic Sulfaquents (INTA 1987).

The regional climate is mesothermic and subhumid, with little or no water deficiency (Burgos and Vidal 1951). The annual precipitation is 809 mm. The annual average temperature is 13.7 °C; the average minimum temperature is 8.1 °C in June, while the average maximum temperature reaches 19.8 °C in January (National Weather Service Mar del Plata, according to the 1920–1980 record 1901–1970).

Most of the study area, except for S-SE sector, is included in the Biosphere Reserve, Man and Biosphere Reserve Program, UNESCO, called "Parque Atlántico Mar Chiquito". This reserve, like other existing in the world, is a coastal ecosystem possessing a variety of sub-environments that host a specific diversity of organisms (Iribarne 2001), and influence complex biogeochemical processes. Mar Chiquita is a shallow body of brackishwater affected by low amplitude tides (Fasano et al. 1982), and constitutes an estuarine environment with a very particular behavior (Marcovecchio et al. 2006).

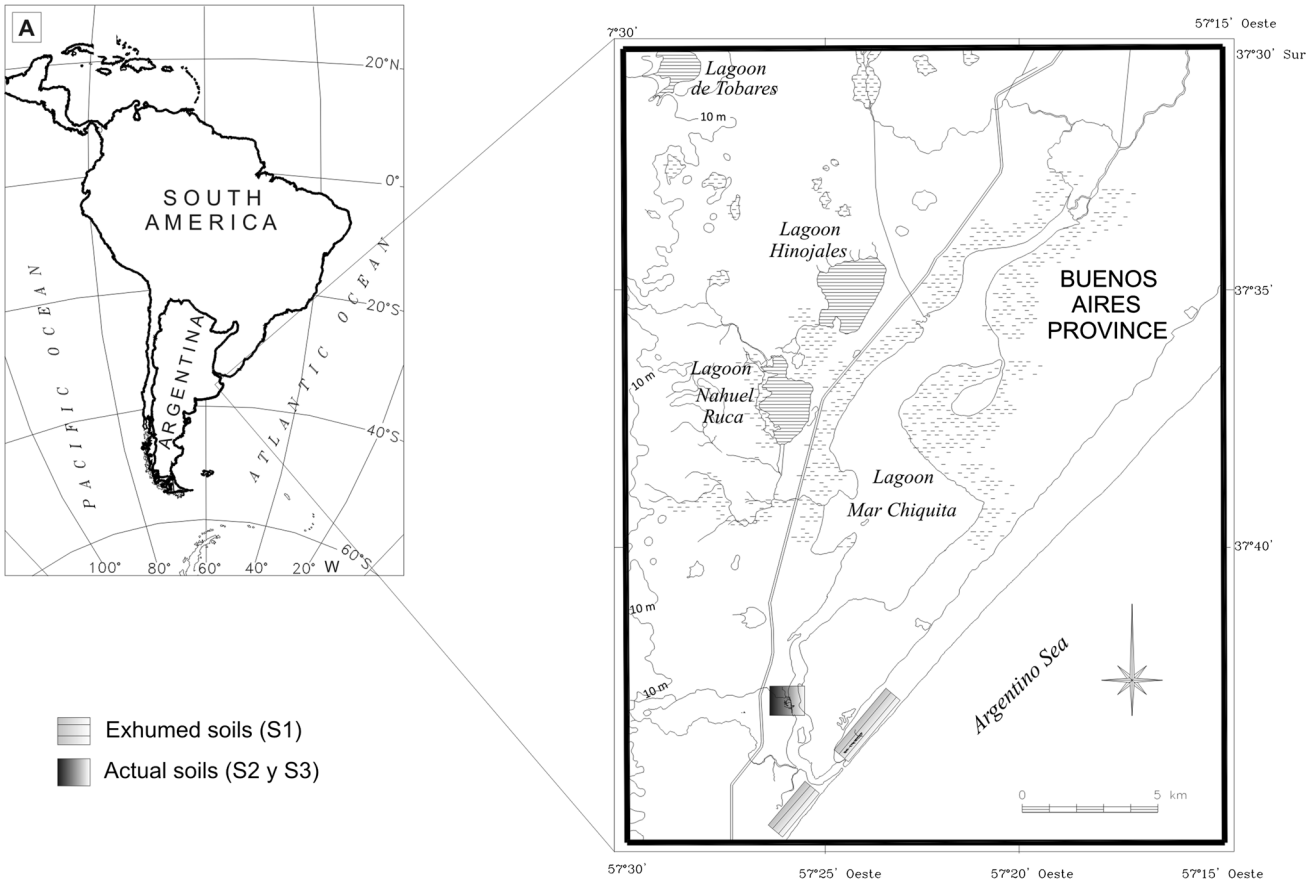

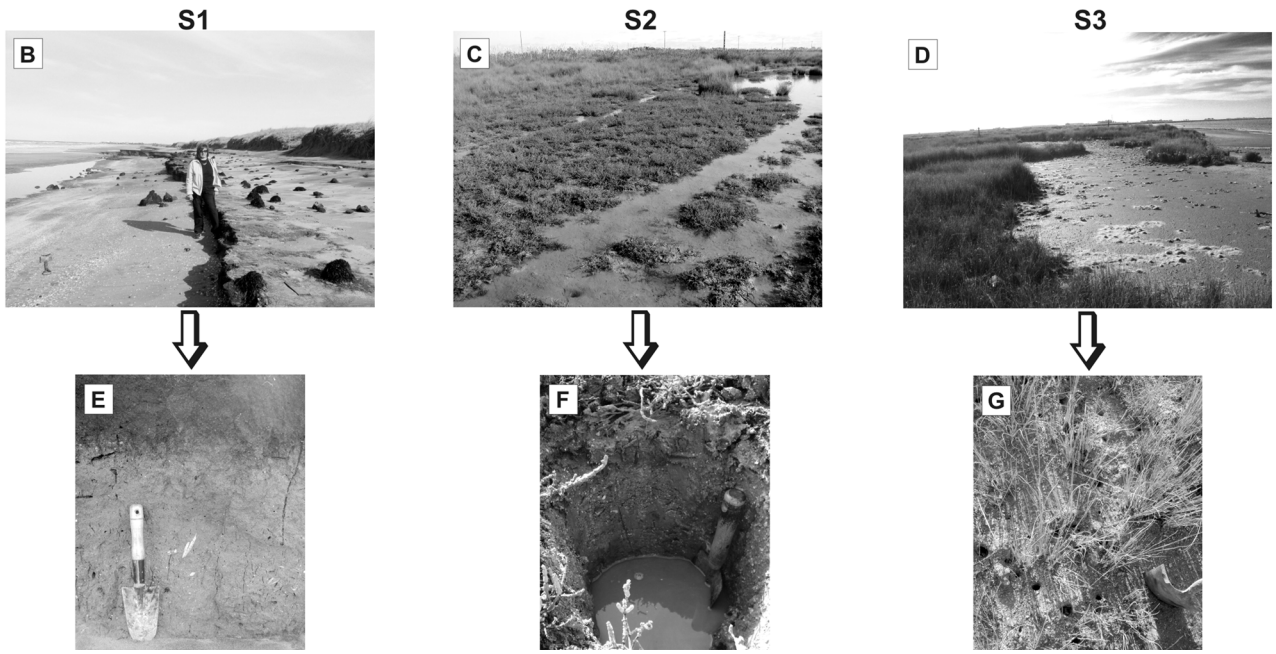

Fig. 1 **a** Map of the location of the study area, **b** Panoramic view of paleosol exhumed in coastal area of Mar Chiquita (S1), **c** Panoramic view of area covered by *Sarcocornia perennis* (S2), **d** Panoramic view of area covered by *Spartina densiflora* (S3), **e** Detail of exhumed paleosol (S1), **f** Detail of actual soil in S2, **g** Detail of actual soil in S3 with crab burrows

The vegetation of the Mar Chiquita coastal lagoon is characterized by psammophytic, halophytic, freshwater and woodlands plant communities, the latter mainly composed of *Celtis ehrenbergiana* (Vervoorst 1967).

Study sites

In the first sampling site (S1), we worked with exhumed soils, which are located on the actual platform of erosion (Fig. 1b, e). The sequence has evolved from ancient coastal deposits, linked to last Holocene transgressive–regressive cycle, and are affected by episodes of storms. The soils are moderately drained, present moderate permeability and are exposed to high levels of erosion. The presence of cracks is commonly observed, besides the precipitation of sodium salts and dissolution of calcium carbonate from bioclastic materials, mainly in the horizons containing plant remains.

In the second sampling site (S2), soils are located within the marginal plain, in micro-depressions linked to ancient tidal channels (Fig. 1c, f). They are affected by the water table very near the surface, remaining saturated for long periods during the rainy seasons and/or affected periodically by the Mar Chiquita coastal lagoon, where iron sulfides are common in the surface. Instead, during dry summers, the presence of cracks and crusts of sodium salts is observed at the surface. These soils are poorly drained, with slow permeability and characterized by the presence of mollusk shells and intensely bioturbated by *Uca uruguayensis* and *Neohelice granulata* (Olivier et al. 1972; Spivak et al. 2001). The predominant vegetation consists of *Sarcocornia perennis* and brackish communities (Isacch et al. 2006) covering approximately 50 % of the surface.

In the third sampling site (S3), the soils have evolved from sand and bioclastic sediments reworked by water action, within the floodplain of the Mar Chiquita coastal lagoon (Fig. 1d, g). They are moderate to fastly drained, with fast permeability detected by the presence of crusts of sodium chloride in dry summers. There is a dense plant cover, predominantly composed of *Spartina densiflora* (Isacch et al. 2006), covering 80 % of the surface.

Methodology

The exhumed soils were analyzed across a section of 12 km length (Fig. 1). The complete soil profile was sampled due to the irregularity given by the storm episodes and ocean erosion. Dating by ^{14}C acceleration mass spectrometry (AMS) were performed (Beta Analytic, USA; LATIR-UNLP) on soil organic matter and bioclastic material (*Tagelus plebeius*) that have been found in life position in the study area. In the actual soils, the first 20 cm of six profiles in each sampling site were analyzed (Fig. 1). Although many soil profiles were studied in all the sampling sites, we report the description of the modal profiles.

Soil morphological description

Morphological profile descriptions were made according to the standards established by the Soil Survey Staff (1996).

Physical and chemical analysis

The soil pH in paste (1:1) was determined with a digital Orion Research 501 pH meter and the organic matter content by the Walkley and Black (1965) method.

To determine soil particle size distribution, samples of each soil horizon were air-dried. About 20 g of each soil sample was treated with 10 % hydrochloric acid and 30 % hydrogen peroxide at 70 °C to eliminate carbonates and oxidize organic matter, respectively. Particle size distribution was determined by pipette analysis (Ingram 1971; Galehouse 1971).

Fresh soil subsamples were used for iron sequential extraction (by a combination of method adapted from Tessier et al. 1979; Huerta-Díaz and Morse 1990; Fortin et al. 1993). The results were expressed in dry weight basis, after correction for water content (61–72 % for all samples) as determined by drying soil subsamples to constant weight. The procedure includes six operationally defined phases (Ferreira et al. 2007):

F1: Exchangeable and soluble Fe: shaken for 30 min in 30 ml of 1 M $MgCl_2$ solution (pH 7.0);
F2: Carbonate-associated Fe: shaken for 5 h in 30 ml of 1 M NaOAc solution (pH 5.0);
F3: Ferrihydrite Fe: shaken for 6 h at 30 °C in 30 ml of 0.04 M hydroxylamine + acetic acid 25 % (vol/vol) solution;
F4: Lepidocrocite Fe: shaken for 6 h at 96 °C in 30 ml of 0.04 M hydroxylamine + acetic acid 25 % (vol/vol) solution;
F5: Crystalline Fe oxides and oxyhydroxides: shaken for 30 min at 75 °C in 20 ml of 0.25 M sodium citrate + 0.11 M sodium bicarbonate solution with 3 g of sodium dithionite;
F6: Pyrite Fe: after a silicate phase (10 M HF extraction) and organic phase (concentrated H_2SO_4 extraction) elimination (Huerta-Díaz and Morse 1990), the pyritic phase was extracted by shaking for 2 h at room temperature in 10 ml of concentrated HNO_3.

The degree of iron pyritization (DOP) was calculated as follows, considering the $\Sigma F1 \rightarrow F5$ as the reactive-Fe phase (Ferreira et al. 2007; Otero et al. 2009; Ferreira et al. 2010):

$$\mathrm{DOP}\ (\%) = [(\mathrm{pyrite} - \mathrm{Fe})/(\mathrm{reactive} - \mathrm{Fe} + \mathrm{pyrite} - \mathrm{Fe})]100$$

Mineralogical and mineralochemical characterization

Once the carbonates and the organic matter were removed from the soil samples, light and heavy minerals were separated by a heavy liquid separation with sodium polytungstate ($3Na_2$-WO_4·$9WO$·H_2O, δ: 2.89 g/cm^3). Light and heavy minerals of the sand fraction: very fine sand (125–62 μm), were mounted with Canada balsam and 400–500 grains per slide were counted under an optical microscope (LeitzWetzlarD35780), polarization microscope (Olimpus BX 51P) and scanning electron microscope (JEOL JSM6460LV). The mineralochemical analyzes were performed using an energy dispersive X-ray spectrometer EDS, between 15 and 25 kV, in undisturbed natural samples.

Results and discussion

Morphological properties

Exhumed soils (S1) presented specific characteristics associated with coastal environment and subsequent active erosion processes, generating several cycles of buried to exhumed soils (Fig. 1b, e). Given this variability, the soils have a low to moderate development, with characteristics of Entisolls and Mollisols (Table 1; Fig. 2). As the palaeosoils classification is very discussed, and in this case soils are affected by the actual coastal morphodynamic with a permanent marine effect; it is considered that these complex sequences that have been diagenized, exhumed and eroded (Buurman 1998), could belong to Hapludolls (A horizons), Sulfaquents (C1 horizons) and Udipsaments and/or Aquents (C2 horizons).

Actual soils have developed from sandy-silt bioclastic parent materials, in a plane environment where microtopographical variations and the degree of saturation have conditioned the evolution of the different soils, showing differences despite the sedimentological homogeneity (Osterrieth 1998). In S2, soils have low development and correspond to Entisolls (haplic Sulfaquents) (Table 1; Figs. 1c, f, 2). In S3, soils have moderate development and belong to Aquolls (aquic Udifluvents) (Table 1; Figs. 1d, g, 2).

Physical and chemical analysis

Organic matter content and pH

Prior to the burial of the exhumed soils, the system functioned as a marsh, generating hydromorphic conditions that slowed the organic matter degradation. This could explain the abundance of plant residues in the sequence and the lower content of organic matter compared with actual soils (Fig. 2). Once the sequence was exposed to oxic conditions and eroded by storm episodes, the oxidation of sulfides and the intense dissolution and transformation of framboidal pyrite into iron crystalline phases could be the responsible for the acidic conditions, mainly in the surface horizons (Fanning et al. 2002) (Fig. 2).

In the actual soils, the content of organic matter decreases with depth and is affected by the plant cover. Despite the sandy texture of the actual soils and their low to moderate pedogenesis, the plant cover (~80 %) in environments associated with *S. densiflora*, has generated horizons with organic matter content similar to other Mollisols in the Pampean Plain (~4–10 %) (Borrelli et al. 2008). These values were two-times higher than those obtained in other sampling sites with smaller plant cover (Fig. 2). These organic matter contents decreased sharply to the parent materials because of the intense transformation and translocation processes that take place in these soils probably in response to the biological activity (Koretsky et al. 2003). The pH values showed quite homogeneous behavior throughout the profile and showed neutral to alkaline values (Fig. 2). Despite the differences in organic matter contents, the pH results may be explained by the saline and/or brackish water influence, also resulting in high exchangeable sodium contents. This acid–base condition may also be related to the composition of the parent materials with abundant bioclastic materials affected by bioerosion processes and reprecipitation of calcium carbonates and oxalates (Osterrieth 2005).

Particle size distribution

In every sampling site analyzed, the soils showed a sandy texture (74–87 %, φ 2–4.5) with scarce pelites (4–9 %, φ 5–11). The results of textural analysis reveal a uni-modal type of distribution, being the fine sands (43–62 %, φ 3–3.5) and very fine sands (27–44 %, φ 4–4.5) the most representative within the sand fraction (Fig. 2).

The dominance of sand fraction, and particularly the very fine sand fraction, is in close relationship with the parent materials from which the soils have evolved. The sandy sediments with abundant bioclastic material would be related to the actual soils while the ancient coastal deposits with the exhumed soils. Moreover, additions processes are very important in these environments, generating not only contributions of fine and very fine materials by wind action; but also by the coastal morphodynamics; mostly by the income of seawater and the effects of the coastal dunes over the exhumed soils. In

Table 1 Morphological characterization of the studied soils

Profile	Horizon	Colour	Texture	Structure	Observations
S1	A	Very dark gray (10YR 3/1) (d) black (10YR 2/1) (w)	Sandy loam	Massive to medium granular; weak, friable, slightly hard, slightly adhesive and non-plastic	Charred remains and bioturbations indicated by the presence of crab burrows
	Cgkb	Light olive (5Y 6/2) (d) olive (5Y 5/3) (w)	Silty-sandy loam	Massive; friable, loose; slightly adhesive and plastic	Abundant whole and fragmented shells, bioturbation signs and decomposed plant residues
S2	A	Very dark brown (10YR 2/2) (d) black (10YR 2/1) (w)	Sandy	Massive; loose, very friable and slightly adhesive	Few bioclastic fragments and abundant roots
	2Cgk1	Olive gray (5Y 5/2) (d) dark gray (5Y 4/1) (w)	Sandy	Massive; loose, non-adhesive nor plastic	Abundant remains of shells, few roots and veins of gley colors
S3	Ak	Dark gray (10YR 4/1) (d) and black (10YR 2/1) (w)	Sandy loam	Moderate granular; soft, very friable, slightly plastic and slightly adhesive	Fragments of bioclastic material, abundant roots and crab bioturbations
	2Ck	light gray (10YR 7/2) (d) gray (10YR 6/1) (w)	Sandy	Massive; soft, very friable, non plastic nor adhesive	Abundant whole and fragmented bioclastic material and crab bioturbations

S1: exhumed soils, S2 and S3: actual soils

actual soils, besides the contributions of fine and very fine materials by wind action, the input of pelites are caused by flooding processes from the Mar Chiquita lagoon, combined with a greater entrapment of material given the increased vegetation cover, especially in environments dominated by *S. densiflora*.

Iron sequential extraction and degree of iron pyritization

The total iron content in the analyzed soils is similar to those reported for other saltmarshes with the same plant cover (Kostka and Luther 1994; Taillefert et al. 2007; Koretsky and Miller 2008); but lower than other similar environments in tropical ecosystems (Ferreira et al. 2007), where the total iron content is fivefold the values observed in these temperate soils.

The average total iron content was 66 ± 11 μmol Fe/g of soil in the exhumed soils and 36–75 μmol Fe/g of soil in the actual soils (Fig. 3). While there were no significant differences in iron contents between all the analyzed soils, the highest content of heavy minerals and their highest degree of weathering in the exhumed soils (Fig. 2), could explain their higher mean iron contents (66 ± 11 μmol Fe/g) when compared to the actual soils (44–60 μmol Fe/g). There was no a clear pattern in the distribution of total iron with depth (Fig. 3). In S2 soils, a tendency of increasing iron with depth was observed. On the other hand, in S3 and the exhumed soils, an homogeneus depth distribution and a decreasing tendency of iron contents with depth were observed, respectively (Fig. 3).

In all the actual and exhumed soils, no iron associated with the exchangeable phase (F1) and carbonate phase (F2) was observed (Fig. 3). The greater proportion of iron remained associated with crystalline oxides and oxyhydroxides (F5, 61–82 %) and lepidocrocite (F4, 13–25 %), and a low proportion to the ferrihydrite phase (F3, 0–9 %) (Fig. 3), as it was reported in other saltmarshes, mainly in the surficial layers of the soils (Luther et al. 1992; Otero and Macias 2003). In these soils, the degree of pyritization (DOP) was low and below the typical values reported for modern estuarine sediments (Wilkin et al. 1996). In the actual soils, DOP did not exceed 3 %, with an average of 1.5 %. On the other hand, the exhumed soils the DOP was greater ranging between 1.2 and 9.4 %.These DOP values are very low compared with other salt marshes where DOP reaches values of about 20–80 % (Kostka and Luther 1994; Otero and Macias 2003) and with analogous tropical environments (15–40 %) (Otero et al. 2009; Nóbrega et al. 2013).

The difference in the iron content and the degree of pyritization between exhumed and actual soils could be explained according to the evolutionary stage of both

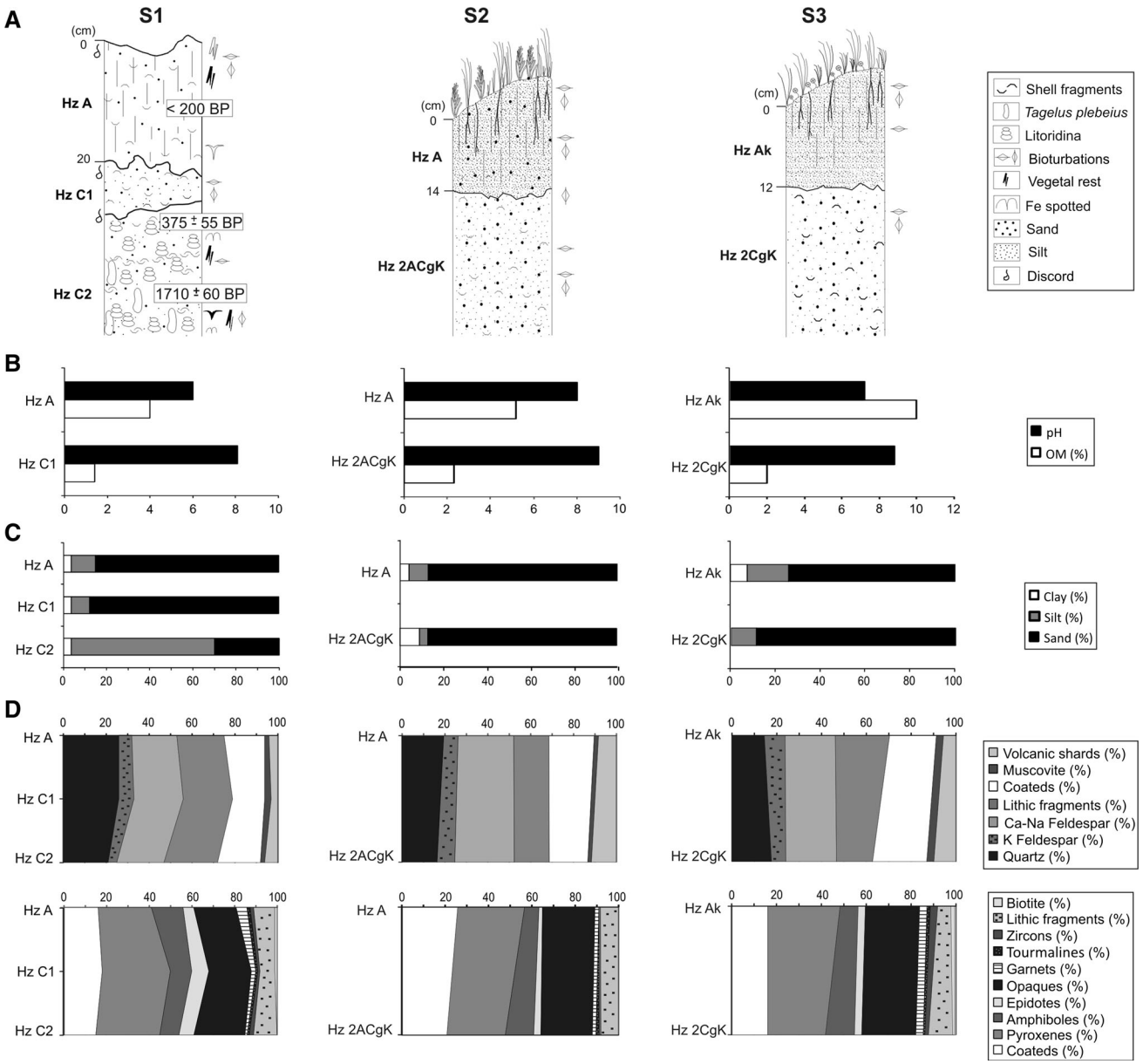

Fig. 2 Morphological, physical and chemical properties of the exhumed (S1) and actual soils (S2, S3) studied. **a** Morphological properties. **b** Organic matter content and pH. **c** Particle size distribution. **d** Light and heavy minerals

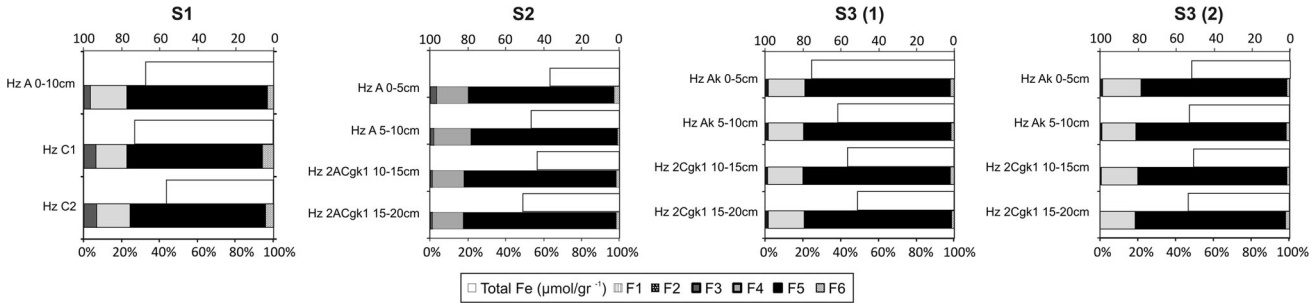

Fig. 3 Total iron content (µmolFe/g^{-1}) and percentages of the geochemical phases of Fe in exhumed (S1) and actual soils (S2, S3). F1: exchangeable. F2: carbonate-bound. F3: ferrihydrite-bound. F4: lepidocrocite-bound. F5: goethite/hematite-bound. F6: pyritic (DOP)

environments. The palaeomarshes have completed their pedological cycle and were buried by the dunes barrier during late Holocene (Osterrieth 1998, 2005). This greater pedological development, compared with actual marshes, has been accompanied by a preservation of framboidal pyrites that, through the exhumation and erosion processes, and oxic conditions, have been only partially weathered.

Another factor to take into account involved in framboidal pyrite preservation is the dissolution of biogenic amorphous silica (diatoms, spicules of Porifera and silicophytoliths) due to the basic conditions of the soils and the presence of halite (Fig. 5a, c). This dissolution process and the subsequent silica precipitation as amorphous gels (Fig. 5c), may have allowed pyrite framboidals to be preserved despite the oxidizing environment to which they have been exposed.

In actual soils, the lower pedological development and the aeration generated by bioturbation and the intense biological activity may have, led to a lower pyritization degree. Particularly, *S. densiflora* has significant underground biomass (7729–7994 gr/m^2) when compared to the aboveground biomass (Bortolus 2006); and crab burrows reach high densities (>60/m^2) with depths that can reach 1 m (Iribarne et al. 1997). This biological activity in the surface levels of the soils would generate intense pyrite oxidation leading to the production and turnover of large amounts of reactive iron oxides that conform the predominance of oxidized iron phase in these soils (Luther et al. 1992; Kostka and Luther 1994; Koretsky et al. 2003; Taillefert et al. 2007; Araújo et al. 2012).

Mineralogical and mineralochemical characterization

Generally, mineralogy is homogeneous in all analyzed soils. The light mineral fraction was mainly composed of minerals coated by oxides, Ca–Na feldspars, quartz and lithic fragments. A low proportion of K feldspar, muscovite and volcanic shards were also present (Fig. 2). The quartz occurs in subangular grains; the plagioclases are limpid to partially coated and weathered; the lithic fragments are mostly weathered or coated and the volcanic shards are clear and some with many oxides and clays in their channels and surfaces (Fig. 2).

The increase of quartz content in the exhumed soils could be related to actual contributions given the intense erosion that prevail in these environments, as well as to the additions of marine materials and to the translocations from the barrier of coastal dunes. The great amount of coated minerals could be explained by the intense iron biogeochemistry, given the oxidation processes of pyrite and its transformation from framboidal pyrite into the predominant iron oxides and oxyhydroxides.

Heavy minerals contents varied among the different soils. Generally, the exhumed soils showed a greater proportion than the actual ones, probably in response to the activity and energy of the erosive agent, given the important marine contributions, storm episodes and the presence of cracks. In the A horizons of the exhumed soils, the content of heavy minerals increases up to 22–42 %wt and decreases in the C horizons to values of 8.5 and 32.2 %wt for the fine and very fine sand fractions, respectively. Pyroxenes, opaque minerals, coated minerals, amphiboles and lithic fragments are the most representative. Garnets, epidotes, tourmalines and zircons do not exceed 5 % (Fig. 2). Exceptionally, tiny specks or irregular black subspherical aggregates are observed at petrographic microscope, which correspond to framboidal pyrite (Figs. 4a, 5a). In the S2 soils, heavy minerals are negligible in the fine sand fraction, and in the very fine sand fraction values of 9–15 %wt arises in the A and C horizons, respectively. In the S3 soils, the content of heavy minerals ranges between 3.6 and 1.8 %wt (A and C horizons, respectively) for the fine sand fraction; and 2.7 %wt in the very fine sand fraction in both horizons.

In order to detail the mineralochemical of the studied soils, aggregates were analyzed (by SEM and EDS) to characterize the matrix components. The analysis of peds of the exhumed soils showed that there is a predominance of silica, iron, sulfur and calcium in the composition of the matrix. In turn, it was observed that the presence, abundance and recurrence of metastable forms of pyrite (mackinawite and greigite), framboidal and poliframboidal pyrite, and isolated octahedral and dodecahedral pyrite closely associated with plant debris, pores and channels of bioclasts (Fig. 4f, h, i, k). The framboids are associated with different types of biofilms mainly of siliceous composition, and have diverse morphologies: combined microcrystals, octahedral–dodecahedral subedrals; irregular octahedral microcrystals subedrals to anedrals, with rounded edges and holes centered; microcrystals with fracture following the crystal structure; loose microcrystals in irregular mass groups, mixed with framboids partially degraded and isolated pyrite microcrystals (Figs. 4g, k, 5b, d–h).

The poliframboids are elongated and subspherical. The subspherical poliframboids have sizes of 55 μm by 65 μm and are immersed in a pure amorphous silica gel, from which emerge framboids leaving the imprint of their individual microcrystals. Elongated poliframboids form clusters of 190 to 140 μm length and 50 to 90 μm wide and are cemented by thin films of amorphous silica and iron (Fig. 5c). Pyrite microcrystals forming framboids are octahedral, dodecahedral, with cubic shapes and sizes of about 0, 2 μm to 5 microns, with a rustic and irregular surface texture. In all cases, framboidal pyrites are

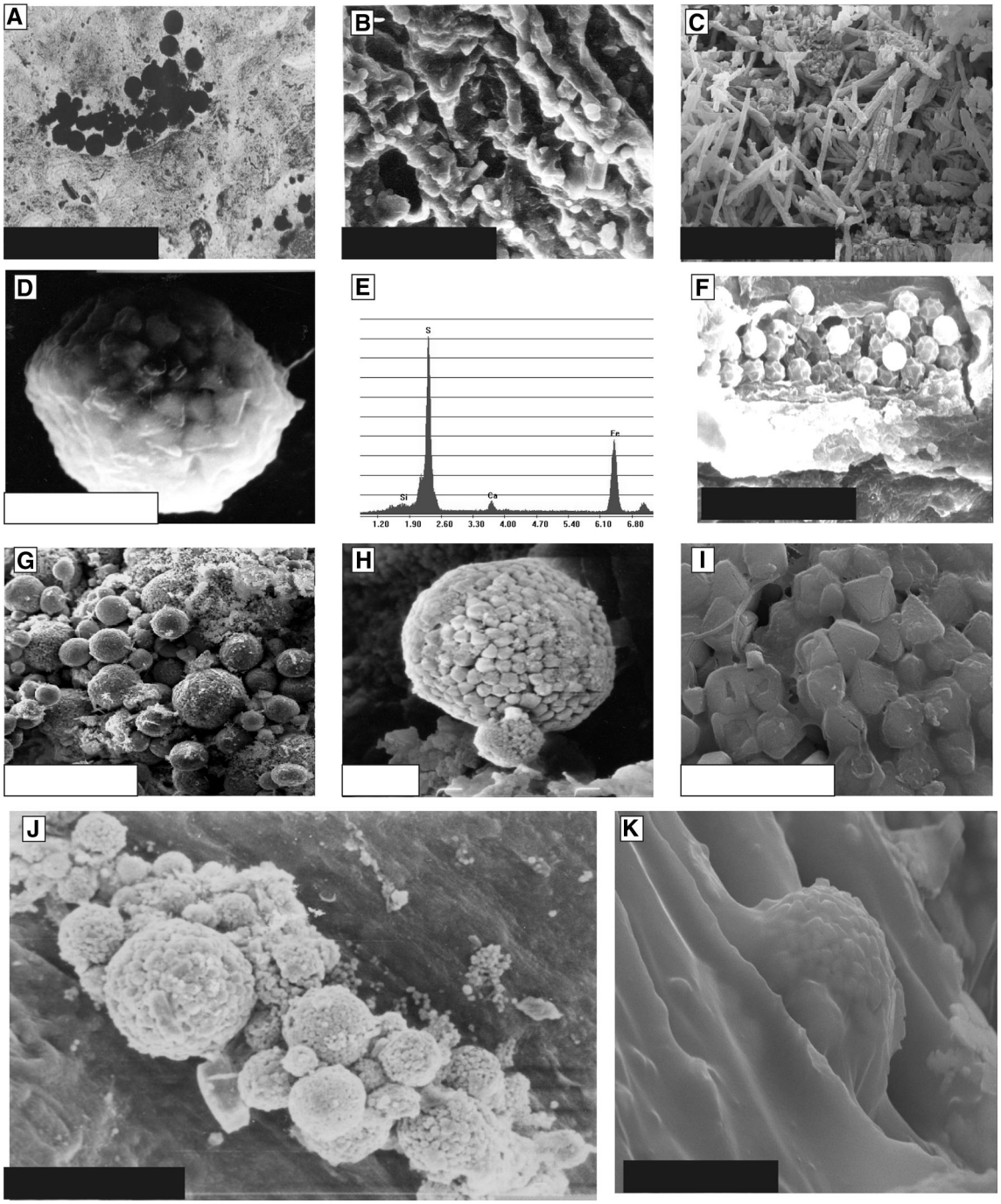

Fig. 4 Exhumed and actual soils. **a** Petrographic view of framboids. **b** Halite in voids on plant remains. **c** Carbonates and calcium oxalates on shells. **d** Greigite with biofilm. **e** EDS of greigite. **f** Dodecahedral pyrite microcrystals on plant remains. **g** Framboidal irregular groups. **h** Little and big pyrite framboids. **i** Octahedral pyrite microcrystals. **j** Elongated poliframboids. **k** Pyrite framboids and biofilm on plant remains. *Scales* **a**–**c**: 100 μm; **d**, **f**, **h**, **i**, **k**: 5 μm; **g**, **j**: 50 μm

authigenic, generated "in situ" under anoxic conditions and, thus, correspond to secondary pyrite (Pons 1965; Osterrieth 1992, 1998). The framboidal pyrite genesis in these coastal soils of the Pampean Plain is bacterial through reduction biogeochemical processes that influence the microcrystals structure, generating clear differences between these biogenic microcrystals and those generated by purely chemical action (Wilkin et al. 1996). The surficial texture of the microcrystals that delineates the framboidal pyrites is rustic and irregular, typical of bacterial activity. Additionally, the semiquantitative analysis of EDAX showed that pyrites were composed of about

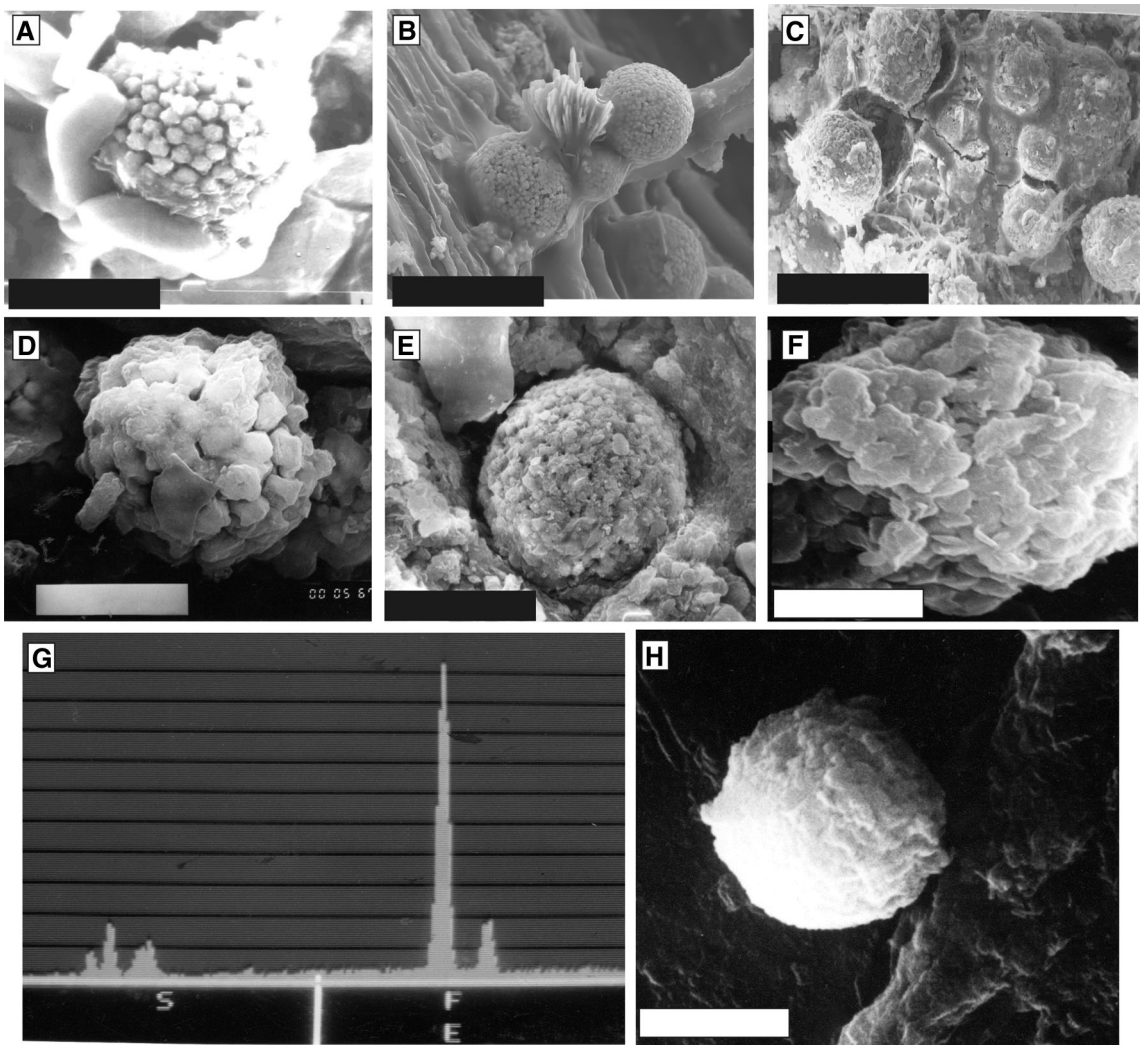

Fig. 5 Exhumed and actual soils. **a** Pyrite framboids coating by halite crystals. **b** Pyrite framboids and gypsum into biofilms on phant remains. **c** Pyrite poliframboid cemented by amorphous silica film. **d**–**f** and **h** Pyrite framboids in different levels of degradation. **g** EDS of H: iron oxyhydroxide. *Scale* 10 μm

38–59 % sulfur and 35–58 % iron (Figs. 4, 5), all values that match the chemical composition of pyrite and its intermediate stages.

Under oxidizing conditions, the well-crystallized pyrites, indicator of their formation in reducing conditions, coexist with barite and gypsum (Fig. 5b), both minerals generated under oxic environments, because of the availability of sulfate and calcium due to degradation of iron sulfides and the intense biogeochemistry associated to bioclasts erosion and reprecipitation of calcium carbonates and oxalates. In both processes, films, coatings or biofilms, as remnants of plant tissues, and/or extracellular polymer products of the metabolic activity of the microorganisms surround the framboids and poliframboids (Polastro 1981). They are a barrier to the diffusion of ions and would be the precursors that produce thin coatings of amorphous silica and Fe hydroxides (Osterrieth 1992, 1998, 2005); promoting coastal sediments stability at the flood plains and sediment protection to the erosion.

Actual soil aggregates have an amorphous matrix predominantly composed of indistinguishable elements and plant remains coated by an amorphous mass. On this mass, cubic crystals of halite of the disdodecahedric class (Fig. 4b) stands out and with a massive-grain structure, partially coating the pores of the aggregates. The EDAX analysis of the mass or amorphous matrix, showed that chlorine is dominant (69.65 %), followed by silica (13.78 %), calcium (5.78 %), iron (4.22 % observed recurrently), sodium (3.74 %) and aluminum (2.79 %). The bioclastic materials are affected by processes of bioerosion and reprecipitation of carbonates and calcium oxalates by action of fungi and algae (Osterrieth 2005). These

compounds were observed on mollusk shells, in the walls of the pores of the aggregates and in the cement of the matrix (Fig. 4c). Despite the presence of iron sulfides detected by the reaction with sodium thiocyanate, the presence of framboidal pyrites has not been observed in these soils; probably due to the dense halophytic vegetation and abundant presence of halite, which does not allow adequate microbial colonization for its genesis (Osterrieth 2005).

Conclusions

In the exhumed and actual soils, biological and pedological processes predominated over sedimentary processes, with a relevant effect of microtopographical variations in a plane environment. Between the biological processes, biomineralization is conspicuous in the soils biogeochemistry, functioning as source of iron, calcium and silicon, which are relevant to the evolution and development of the soils. In turn, between the pedological processes, additions, transformations and transfers predominate over removals.

Biofilms detected in the exhumed soils are recurrent, multifunctional and the product of intense microbial activity. They promote the conservation and persistence of framboidal pyrite and help to form flocs that determine the persistence of pedosedimentary levels even in highly erosive conditions.

It have been defined anoxic pulses that generated acidic media, even in the persistent exhumed soils, which would indicate retreat of the sea and production of highly aggressive sulfuricization process, which would have caused the degradation of the brackish paleomarsh, mineral alteration and the possible destruction of calcareous microfossils.

The study of soil biogeochemistry in palaeomarshes contributes to the understanding of the pedological and biogeochemical processes of iron in actual soil marshes. The presence and persistence of secondary framboidal pyrite indicates a prevalence and persistence of reducing conditions linked to the sea advance during the evolution of the palaeomarsh. Besides, the presence of framboidal pyrite, Fe oxides and oxyhydroxides in the coastal exhumed soils of southeast Buenos Aires, constitute an example of the complex biogeochemistry produced in humid temperate palaeomarshes. This situation could have been repeated before the transgressive–regressive processes on the actual marshes and/or in response to an inadequate anthropic management, with serious and irreversible environmental problems.

Acknowledgements This study was financially supported by Mar del Plata National University (EXA 741/15), National Agency for Science and Technology Promotion (ANPCyT, BID PICT No 1583), CONICET (PIP 112-20130100145CO) and MINCyT-CAPES (BR/09/13, BR/RED/14/14). The authors thank to Ing. José Vila for their assistance with SEM and EDS analysis.

References

Araújo JMC Jr, Otero XL, Marques AGB, Nóbrega GN, Silva JRF, Ferreira TO (2012) Selective geochemistry of iron in mangrove soils in a semiarid tropical climate: effects of the burrowing activity of the crabs *Ucides cordatus* and *Uca maracoani*. Geo Mar Lett 32(4):289–300

Berner RA (1970) Sedimentary pyrite formation. Am J Sci 268:1–23

Berner RA (1982) Burial of organic carbon and pyrite sulfur in modern ocean: its geochemical and environmental significance. Am J Sci 282:451–473

Berner RA (1984) Sedimentary pyrite formation: an update. Geochim et Cosmochim Acta 48:605–615

Bianchi TS (2006) Biogeochemistry of estuaries. Oxford University Press, Oxford

Borrelli N, Osterrieth M, Marcovecchio J (2008) Interrelations of vegetal cover, silicophytolith content and pedogenesis of typical Argiudolls of the Pampean Plain, Argentina. Catena 75(2):146–153

Bortolus A (2006) The austral cordgrass Spartina densiflora Brong: its taxonomy, biogeography and natural history. J Biogeogr 33:158–168

Burgos JJ, Vidal AL (1951) Los climas de la República Argentina, según la nueva clasificación de Tornthwaite. Meteoros 1(1):3–32

Buurman P (1998) Classification of paleosols—a comment. Quat Int 51/52(7/8):17–33

Duarte CM, Middelburg JJ, Caraco N (2005) Major role of marine vegetation on the oceanic carbon cycle. Biogeosciences 2:1–8

Fanning M, Rabenhorst M, Burch S, Islam K, Tangren S (2002) Sulfides and sulfates. In: Dixon and Schulze (eds). Soil mineralogy with enviromental application. SSSA Book Series 7 7: 229–261

Fasano JL, Hernández MA, Isla FI, Schnack EJ (1982) Aspectos evolutivos y ambientales de la Laguna Mar Chiquita (Provincia de Buenos Aires, Argentina). Oceanologica Acta, 285–292 **(Special Publication)**

Ferreira TO, Vidal-Torrado P, Otero XL, Macías F (2007) Are mangrove forest substrates sediments or soils? A case study in southeastern Brazil. Catena 70:79–91

Ferreira TO, Otero XL, Souza VS Jr, Vidal-Torrado P, Macías F, Firme LP (2010) Spatial patterns of soil attributes and components in a mangrove system in Southeast Brazil (São Paulo). J Soils Sediments 10:995–1006

Ferreira TO, Nóbrega GN, Albuquerque AGBM, Sartor LR, Gomes IS, Artur AG, Otero XL (2015) Pyrite as a proxy for the identification of former coastal lagoons in semiarid NE Brazil. GeoMar Lett 35:355–366

Fortin D, Leppard GG, Tessier A (1993) Characteristics of lacustrine diagenetic iron oxyhydroxides. Geochim Cosmochim Acta 57:4391–4404

Frenguelli J (1950) Rasgos generales de la morfología y la geología de la Provincia de Buenos Aires. Lemit 2(33):72

Galehouse JS (1971) Sedimentation analysis. In: Carver (ed) Procedures in sedimentary petrology. Wiley Interscience, USA, pp 69–94

Henderson GM (2002) New oceanic proxies for paleoclimate. Earth Planet Sci Lett 203:1–13

Howarth RW (1984) The ecological significance of sulfur in the energy of salt marsh and coastal marine sediments. Biogeochemistry 1:5–27

Huerta-Díaz MA, Morse JW (1990) A quantitative method for determination of trace metals in sedimentary pyrite. Mar Chem 29:119–144

Ingram RL (1971) Sieve analysis. In: Carver (ed) Procedures in sedimentary petrology. Wiley Interscience, USA, pp 41–68

INTA (1987) Unidad de Recurso de Suelos: Mapa geomorfológico y de suelos de la Provincia de Buenos Aires. Escala 1:50.000. Castelar

Iribarne OO (ed) (2001) Reserva de Biosfera Mar Chiquita: Características físicas, biológicas y ecológicas. Ed Martín, Mar del Plata, Argentina

Iribarne OO, Bortolus A, Botto F (1997) Between-habitat differences in burrow characteristics and trophic modes in the southwestern Atlantic burrowing crab *Chasmagnathus granulata*. Mar Ecol Prog Ser 155:132–145

Isacch JP, Costa CSB, Rodríguez-Gallego L, Conde D, Escapa M, Gagliardini DA, Iribarne OO (2006) Distribution of saltmarsh plant communities associated with environmental factors along a latitudinal gradient in the south-west Atlantic coast. J Biogeogr 3:888–900

Isla FI, Fasano JL, Ferrero L, Espinosa M, Schnack EJ (1988) Late Cuaternary marine-estuarine sequences of the Southeastern coast of Buenos Aires Province, Argentina. Quat S Am Ant Pen 6:137–157

Koretsky CM, Miller D (2008) Seasonal influence of the needle rush Juncus roemerianus on saltmarsh porewater geochemistry. Estuaries Coast 31:70–84

Koretsky CM, Moore CM, Lowe KL, Meile C, Dichristina TJ, van Cappellen P (2003) Seasonal oscillation of microbial iron and sulfate reduction in saltmarsh sediments (Sapelo Island, GA, USA). Biogeochemistry 64:179–203

Kostka JE, Luther GW III (1994) Partitioning and speciation of solid phase iron in saltmarsh sediments. Geochim et Cosmochim Acta 58(7):1701–1710

Lovley DR (2000) Environmental microbe-mineral interactions. ASM Press, Washington

Lowenstam HA (1981) Minerals formed by organisms. Science 211:1126–1131

Luther GW III, Kostka JE, Church TM, Sulzberger B, Stumm W (1992) Seasonal iron cycling in the salt-marsh sedimentary environment: the importance of Fe(II) and Fe(III) in the dissolution of Fe(III) minerals and pyrite, respectively. Mar Chem 40:81–103

Marcovecchio J, Freije H, De Marco S, Gavio MA, Ferrer L, Andrade S, Beltrame O, Asteasuain R (2006) Seasonality of hydrographic variables in a coastal lagoon: Mar Chiquita, Argentina. Aquat Conserv Mar Freshw Ecosyst 16:335–347

Morse JW, Millero FJ, Cornwell JC, Rickard D (1987) The chemistry of the hydrogen sulfide and iron sulfide systems in natural waters. Earth Sci Rev 24:1–42

Nóbrega GN, Ferreira TO, Romero RE, Marques AGB, Otero XL (2013) Iron and sulfur geochemistry in semi-arid mangrove soils (Ceará, Brazil) in relation to seasonal changes and shrimp farming effluents. Environ Monit Assess 185(9):393–7407

Odum EP (1970) Fundamentals of ecology. Saunders, USA

Olivier S, Escofet AM, Penchaszadeh P, Orenzanz JM (1972) Estudios ecológicos de la región estuarial de Mar Chiquita (Buenos Aires, Argentina). Las comunidades bentónicas. Anal Com Inv Cient 193(5–6):237–262

Osterrieth M (1992) Pirita framboidal en secuencias sedimentarias del Holoceno tardío en Mar Chiquita, Buenos Aires, Argentina. In: IV Reunión Argentina de Sedimentología 2: 73–80

Osterrieth M (1998) Paleosols and their relation to sea level changes during the Late Quaternary in Mar Chiquita, Buenos Aires, Argentina. Quatern Int 51–52:43–44

Osterrieth M (2005) Biomineralizaciones de hierro y calcio, su rol en procesos biogeoquímicos de secuencias sedimentarias del sudeste bonaerense. In: XVI Congreso Geológico Argentino III: 255–262

Otero XL, Macias F (2003) Spatial variation in pyritization of trace metals in salt-marsh soils. Biogeochemistry 62:59–86

Otero XL, Ferreira TO, Vidal-Torrado P, Macías F (2006) Spatial variation in pore water geochemistry in a mangrove system (Pai Matos island, Cananeia–Brazil). Appl Geochem 21:2171–2186

Otero XL, Ferreira TO, Huerta-Díaz MA, Partiti CSM, Souza V Jr, Vidal-Torrado P, Macías F (2009) Geochemistry of iron and manganese in soils and sediments of a mangrove system, Island of Pai Matos (Cananeia–SP, Brazil). Geoderma 148:318–335

Polastro RM (1981) Authigenic kaolinite and associated pyrite in chalk of the Creaceous Niobrara formation, eastern Colorado. J Sed Petrol 5(1,2):553–562

Pons LJ (1965) A quantitative microscopical method of pyrite determination in soils. In: Jorgerius A (ed) Proc Microm Symp 401–409

Raiswell R, Berner RA (1985) Pyrite formation in euxinic and semi-euxinic sediments. Am J Sci 285:710–724

Roychoudhury A, Kostka J, Van Cappellen P (2003) Pyritization: a palaeoenvironmental and redox proxy reevaluated. Estuar Coast Shelf Sci 57:1183–1193

Schnack EJ, Gardenal M (1979) Holocene transgressive deposits, Mar Chiquita lagoon coast, Buenos Aires province, Argentina. Proc Int Symp Coast Evol Quat, Sao Paulo, pp 419–425

Simonson RW (1959) Outline of a generalizade theoryof soil genesis. Soil Sci Soc Am Proc 23:152–156

Soil Survey Staff (1996) Keys to soil taxonomy, 7th edn. United States Department of Agriculture, Washington

Spivak E, Luppi T, Bas C (2001) Cangrejos y camarones: las relaciones organismo-ambiente en las distintas fases del ciclo de vida. In: Iribarne O (ed) Reserva de la biosfera Mar Chiquita: características físicas, biológicas y ecológicas, Ed Martin, Mar del Plata, Argentina, pp 129–152

Stribling J (1997) The relative importance of sulfate availability in the growth of *Spartina alterniflora* and *Spartina cynosuroides*. Aquat Bot 56:131–143

Taillefert M, Neubhuber S, Bristow G (2007) The effect of tidal forcing on biogeochemical processes in intertidal salt marsh sediments. Geochem Trans 8:6

Tessier A, Campbell PGC, Bisso M (1979) Sequencial extraction procedure for the speciation of particulate trace metals. Anal Chem 5:844–855

Tobias C, Neubauer SC (2009) Salt marsh biogeochemistry—an overview. In: Perillo GME, Wolansky E, Cahoon DR, Brinson MM (eds) Coastal wetlands. An integrated ecosystem approach, Elsevier, Amsterdam, The Netherlands, pp 445–492

Tricart JL (1973) Geomorfología de la Pampa Deprimida. INTA 12:202

Vervoorst F (1967) La vegetación de la República Argentina Vll. Las comunidades vegetales de la depresión del Salado (Pcia de BsAs). INTA Serie Fitogeográfica 7:24

Viaroli P, Laserre P, Campostrini P (2007) Lagoons and coastal wetlands. Hidrobiología 577:1–3

Violante RA, Parker G, Cavallotto JL (2001) Evolución de las llanuras costeras del este bonaerense entre la bahía Samborombón y la laguna Mar Chiquita durante el Holoceno. Revista de la Asociación Geológica Argentina 56:51–66

Walkley Black (1965). In: Black C (ed) Methods of Soil Analysis. American Society of Agronomy, pp 1372–1375

Wilkin RT, Barnes HL, Brantley SL (1996) The size distribution of framboidal pyrite in modern sediments: an indicator of redox conditions. Geochim et Cosmochim Acta 60(20):3897–3912